engineering proceedings

MDPI

Proceeding Paper

Fabrication of Aluminum-Based Hybrid Nanocomposite for Photocatalytic Degradation of Methylene Blue Dye: A Techno-Economic Approach †

Samuel Demarema [1], Amal Abdelhaleem [1,*], Shinichi Ookawara [2] and Mahmoud Nasr [1,3,*]

1 Environmental Engineering Department, Egypt-Japan University of Science and Technology (E-JUST), 21934 Alexandria, Egypt; samuel.demarema@ejust.edu.eg
2 Department of Chemical Science and Engineering, Tokyo Institute of Technology, Meguro-ku, Tokyo 152-8552, Japan; ookawara.s.aa@m.titech.ac.jp
3 Sanitary Engineering Department, Faculty of Engineering, Alexandria University, Alexandria 21544, Egypt
* Correspondence: amal.elsonbaty@ejust.edu.eg (A.A.); mahmoud.nasr@just.edu.eg (M.N.)
† Presented at the 2nd International Electronic Conference on Processes: Process Engineering—Current State and Future Trends (ECP 2023), 17–31 May 2023; Available online: https://ecp2023.sciforum.net/.

Abstract: Al_2O_3-MgO nanocomposite was synthesized using co-precipitation method for photocatalytic degradation of methylene blue (MB) dye under UV-vis light. Box benken design (BBD) in response surface methodology (RSM) was used for optimization and modelling of the photocatalytic degradation of MB dye. Analysis of variance (ANOVA) revealed a quadratic model with R^2 of 0.9880. MB removal followed first order kinetic model (R^2 = 0.9520, k_1 = 0.007 min^{-1}). Economic feasibility study at optimized conditions showed that the wastewater treatment cost is US$ 16.50/m^3 and payback period is 3.17 years.

Keywords: photo-degradation mechanism; dye-laden solution; kinetic model; optimum operating condition; running cost

Citation: Demarema, S.; Abdelhaleem, A.; Ookawara, S.; Nasr, M. Fabrication of Aluminum-Based Hybrid Nanocomposite for Photocatalytic Degradation of Methylene Blue Dye: A Techno-Economic Approach. *Eng. Proc.* **2023**, *37*, x. https://doi.org/10.3390/xxxxx
Published: 17 May 2023

1. Introduction

Methylene blue (MB) is a highly toxic cationic dye widely used in textile, pharmaceutical and printing industries. Exposure to MB dye results in physiological disorders leading to acute and chronic illness such as vomiting, eye irritation and jaundice [1,2].The discharge of MB laden wastewater has detrimental effects on aquatic biota. MB changes aesthetics of aquatic systems leading to low sunlight available for photosynthesis resulting in stunted growth and death of aquatic plants. MB dye forms complex products in aqueous systems leading to low dissolved oxygen and death of aquatic organisms, resulting in loss of biodiversity in marine ecosystem[2].

MB dye can be removed by conventional wastewater treatment methods such as adsorption, coagulation, and phytoremediation [1]. However, the major drawback of conventional systems is the formation of secondary pollutants. Additionally, there is a high cost of regeneration of adsorbents and disposal of pollutant laden sludge [3].

Currently, advanced oxidation processes (AOPs) have been adopted for the degradation of organic pollutants by utilizing highly reactive hydroxyl radicals [4]. AOPs such as photocatalysis and photo-Fenton reaction can degrade MB dye into smaller and non-toxic molecules [3]. Due to high stability and efficiency of TiO_2 and ZnO nano semiconductors, they are widely used in photodegradation of organic dyes [4].

Al_2O_3 has high thermal stability, large surface area and well defined nanopore structures [5]. It is widely used in sensors, energy storage and pharmaceutical applications [6]. Al_2O_3 has significant optical properties, hence it can be used as a photocatalyst [5]. Al_2O_3

can be synthesized from abundant waste aluminum cans [7], resulting in lower economic costs as comparison to TiO_2 and ZnO.

Al_2O_3 has a relatively high band gap energy of 5.97 eV [8], hence lower photocatalytic activity. To improve photocatalytic efficiency, Al_2O_3 can be combined with MgO to form a nanocomposite. MgO has large surface area and structural defects that allow for generation of reactive radicals under UV radiation [9]. MgO can form heterojunction with Al_2O_3 to have lower the band gap energy, with respect to that of Al_2O_3. This leads to improved photocatalytic degradation efficiency.

This study focuses on synthesis of Al_2O_3-MgO nanocomposite using co -precipitation for photodegradation of MB dye. The effect of operating parameters in MB photodegradation is investigated. An economic feasibility analysis is carried out to assess the costs of photocatalytic degradation of MB using Al_2O_3-MgO.

2. Materials and Methods

2.1. Materials

Aluminum nitrate nonahydrate ($Al(NO_3)_3.9H_2O$) was purchased from Qualikems Fine Chem Ltd., India. Magnesium chloride hexahydrate ($MgCl_2.6H_2O$) was purchased from Tekkim, Turkey. Methylene blue ($C_{16}H_{18}ClN_3S$, 99%) was bought from Alpha Chemical group, Egypt. Methanol (CH_3OH, 99.8%) and sulphuric acid (H_2SO_4, 97%) were purchased from Piochem, Egypt. Sodium hydroxide pellets (NaOH, 97%) were bought SD fine Chem Ltd., India.

2.2. Photocatalyst Synthesis

The photocatalyst was prepared via a simple co-precipitation technique [8] as shown in Figure S1. Briefly, 0.2 M $Al(NO_3)_3.9H_2O$ was mixed with 0.2 M $MgCl_2.6H_2O$ and 1 M NaOH was added dropwise until pH was 11. A white precipitate is formed with constant stirring for 30 min. The precipitate was washed with distilled water, filtered, dried for 12 h at 105 °C and finally calcined at 800 °C for 3 h to get Al_2O_3-MgO nanocomposite.

2.3. Characterization

The optical band gap energy was measured using Jasco V-570 UV-DRS spectrophotometer in the range 220–2000 nm. The point of zero charge was determined using the batch equilibrium method [4].

2.4. Experimental Setup

A stock solution of 50 ppm of methylene blue solution was prepared by dissolving 50 mg of methylene blue dye in 1L of distilled water. The required solutions were prepared using the stock solution. Photodegradation of MB dye was carried out in a photoreactor with a 400 W metal halide lamp. The pH of MB dye solution was adjusted using 1 M NaOH or 1 M H_2SO_4. The experiment was initially run in the dark for 60 min to achieve adsorption-desorption equilibrium. The concentration of MB after adsorption (C_o) was measured at 664 nm using UV spectrophotometer (Jasco V-630 spectrophotometer, Japan). The light was turned on to initiate photocatalytic degradation. After photodegradation, samples of MB were withdrawn, quenched with methanol and centrifuged at 6000 rpm. The final concentration of MB (C_f) was measured. MB removal was calculated using Equation (1).

$$\text{MB removal} = [(C_o - C_f)/C_o] \times 100 \quad (1)$$

The experimental conditions in Table 1 are derived from BBD in RSM.

Table 1. Experimental factors and limits in BBD.

Factor	Parameter	Unit	Levels		
			Low	Median	High
A	pH	-	3	7	11
B	Time	min	60	120	180
C	Photocatalyst dosage	mg/L	200	600	1000
D	Initial MB dye concentration	ppm	10	55	100

2.5. Statistical Analysis

Experimental results were analyzed by Response Surface Methodology (RSM) and one way ANOVA analysis in Design Expert 13.

3. Results and Discussion

3.1. Material Characterization

Al_2O_3-MgO was characterized using UV-DRS. Figure 1a shows the plot of absorbance and wavelength for Al_2O_3-MgO. The maximum absorbance of Al_2O_3-MgO was at 290 nm.

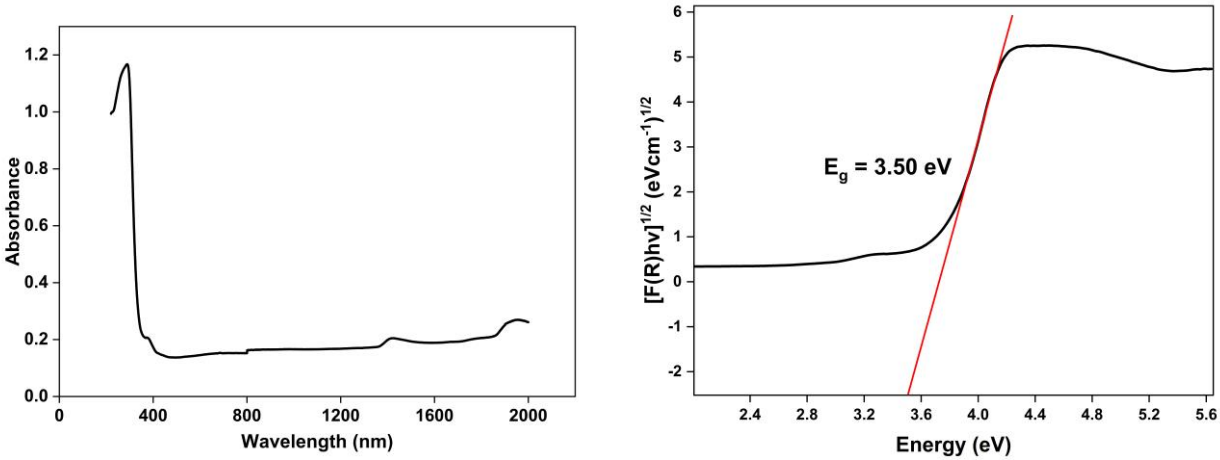

(**a**) (**b**)

Figure 1. UV-DRS (**a**) Absorbance and (**b**) Kubelka-Munk plots for Al_2O_3-MgO.

The band gap of Al_2O_3-MgO was calculated from the Kubelka- Munk function [F(R)] using the Tauc equation as shown in Equation (2) [10].

$$[[F(R)hv]^{(1/\gamma)} = B(hv - E_g) \quad (2)$$

where h is the Planck's constant, v is frequency of the photon, B is constant and E_g is the band gap energy of Al_2O_3-MgO. γ is equal to 2 for indirect band gap transition [10]. From the Kubelka-Munk plot in Figure 1a, the E_g for Al_2O_3-MgO is 3.50 eV. The E_g for pure Al_2O_3 is reported to be 5.97 eV [8]. Al_2O_3-MgO has lower E_g than pure Al_2O_3 due to presence of defects and heterojunction in the Al_2O_3-MgO nanocomposite [6,11].

3.2. Initial Photocatalyst Tests and Effect of Operational Parameters

Figure 2a shows the photodegradation tests of 11 ppm MB dye with pH, time and photocatalyst dosage as 7, 180 min and 500 mg/L respectively. Pure Al_2O_3 had photodegradation efficiency of 43.57% whereas Al_2O_3-MgO had 72.72%. Al_2O_3-MgO has lower band gap energy than Al_2O_3 hence higher photocatalytic activity.

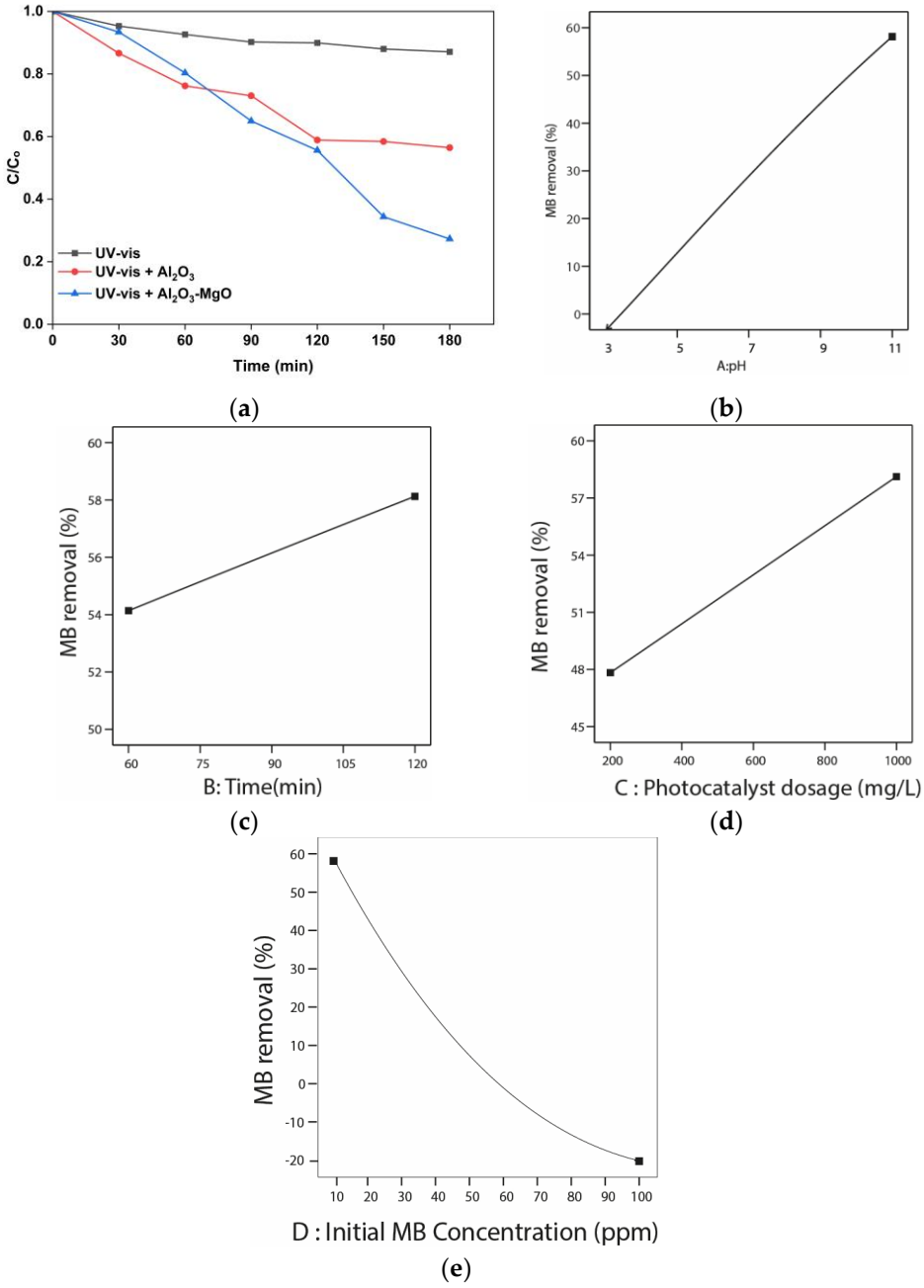

Figure 2. (**a**) Initial photocatalyst test; Effect of (**b**) pH; (**c**) time; (**d**) photocatalyst dosage; (**e**) initial MB dye concentration on MB photodegradation.

The effect of pH is shown in Figure 2b. As pH increased from 3 to 11, MB removal increased from 0% to 57%. In acidic pH, MB exists as a neutral molecule below its pKa value of 3.8 [12]. The point of zero charge (pH_{zc}) of Al_2O_3-MgO is 10.04, as shown in Figure S2. In acidic conditions, surface of Al_2O_3-MgO is positively charged and MB molecules have low adsorption on catalyst surface, leading to low photodegradation efficiency. MB dye exists as cations above the pKa value. As the pH approaches the $pH_{zc,}$ the repulsive force against MB cations is reduced [13]. In alkaline conditions, above the pH_{zc}, surface of Al_2O_3-MgO is negatively charged and attracts the MB cations. This leads to uptake of photogenerated holes and electrons leading to higher photodegradation efficiency.

Figure 2c shows the effect of time on photodegradation of MB dye. MB removal increased from 54% at time of 60 min to 58% at time of 180 min. At constant photocatalyst dosage, more electrons and holes are generated by Al_2O_3-MgO as irradiation time

increases. This leads to production of more reactive radical species, leading to an increment in the photocatalytic degradation efficiency [14].

The effect of photocatalyst dosage is shown in Figure 2d. MB removal increased from 48% at 200 mg/L to 58% at 1000 mg/L. Increasing Al_2O_3-MgO dosage leads to the generation of more active sites and subsequently leads to higher photodegradation efficiency for MB degradation [11]. However, high Al_2O_3-MgO dosage causes agglomeration of particles. This results in low photon uptake by Al_2O_3-MgO and low generation of electrons and holes hence decrease in MB photodegradation efficiency [15].

The effect of initial MB dye concentration is shown in Figure 2e. MB removal was reduced from 57% to 0% as initial MB dye increased from 10 to 100 ppm. As concentration of MB dye increases, more MB molecules are adsorbed on surface of Al_2O_3-MgO. This limits the influx of photons on the photocatalyst surface, resulting in low generation of electrons and holes [11]. At constant Al_2O_3-MgO dosage and light radiation, the amount of reactive radicals generated is insufficient for MB photodegradation. Intermediates will also compete with parent MB molecule for radicals, leading to lower photodegradation efficiency.

Figure S3 shows the 3D contour plots for interaction of parameters. Each individual parameter contributes to achieve MB photodegradation.

3.3. Optimization of Operational Factors

$$(\text{MB removal} + 22.5)^{0.81} = 12.63 + 1.56A - 0.9753B + 0.4529C - 5.39D + 1.97AB + 0.3677AC - 10.15AD - 14.3BD - 1.01CD - 1.38A^2 - 0.0321B^2 - 0.0093C^2 + 4.86D^2 \quad (3)$$

3.4. Model Validation and Kinetics

The optimized conditions of pH, time, photocatalyst dosage and initial MB concentration were 11, 115.6 min, 996.846 mg/L and 10 ppm respectively, resulting in MB dye removal of 57.82% as shown in Figure S4a. The verification experiment at optimized conditions revealed that MB removal was 59.20% as shown in Figure S4b, with an error of 1.68%. The photodegradation of MB dye with Al_2O_3-MgO followed first order kinetics with R^2 of 0.9520 and k_1 as 0.007 min^{-1} as shown in Figure S5.

3.5. Suggested Removal Mechanism

The mechanism for MB degradation by Al_2O_3-MgO is shown in Figure S6. It is assumed MB degradation is due to attack of generated hydroxyl (OH•) and superoxide (O_2-•) radicals. The radicals are generated when photon of light is incident on Al_2O_3-MgO leading to excitation of electrons from the valence band (VB) to the conductance band (CB). This leads to generation of holes (h^+_{VB}) and electrons (e^-_{CB}). Hydroxyl ions from water will react with holes to produce OH•. Oxygen present in the MB solution reacts with electrons to produce O_2-•. The radicals will react with MB dye molecules resulting in degradation products, carbon dioxide and water. Equations (3)–(7) summarize the degradation mechanism [10,12].

$$Al_2O_3\text{-MgO} + hv \text{ (vis region)} \rightarrow Al_2O_3\text{-MgO} (e_{cb}^- + h_{vb}^+) \quad (3)$$

$$h_{vb}^+ + H_2O(OH\text{-}) \rightarrow OH\bullet + H^+ \quad (4)$$

$$e_{cb}^- + O_2 \rightarrow O_2^-\bullet \quad (5)$$

$$O_2^-\bullet + MB \rightarrow \text{degradation products} + CO_2 + H_2O \quad (6)$$

$$OH\bullet + MB \rightarrow \text{degradation products} + CO_2 + H_2O \quad (7)$$

3.6. Economic Evaluation

An economic evaluation for synthesis of Al_2O_3-MgO and application in photodegradation of MB dye was conducted. The textile wastewater treatment plant was assumed to be treating 80 m^3 of wastewater per day under optimized conditions. The annual operating time was 300 days. **Error! Reference source not found.**S3 summarizes the economic evaluation. The amortization cost (A) was calculated using Equation S5 [15] for a period of 25 years at an interest rate of 6% per annum and was found to be US$ 365,765.78. The annual cost (AC) of treating textile wastewater cost per m^3 was evaluated using Equation (S6). For 300 working days, the AC was US$ 16.50/m^3. The revenue generated from sales of Al_2O_3-MgO nanocomposite was calculated as US$ 3.25/m^3 of treated wastewater. Wastewater recycling and pollution reduction were US$ 0.46/m^3 and US$ 0.16/m^3, respectively. The payback period was 3.17 years as shown in text S1.

3.7. Conclusions

An Al_2O_3-MgO nanocomposite was prepared using the co-precipitation method. UV-DRS analysis showed that the band gap energy was 3.50 eV. Al_2O_3-MgO nanocomposite was used in photocatalytic degradation of MB dye. The effect of operating parameters was investigated using RSM. The RSM model had R^2 of 0.9880, indicating good prediction of MB removal. MB photocatalytic degradation using Al_2O_3-MgO followed first order kinetics. Economic estimation revealed that the wastewater treatment cost was US$ 16.50/m^3 with a payback period of 3.17 years.

Supplementary Materials: The following supporting information can be downloaded at: www.mdpi.com/xxx/s1. Figure S1: Synthesis of Al_2O_3-MgO; Figure S2: pH_{zc} of Al_2O_3-MgO; Figure S3: 3D contour plots for interaction of parameters; Table S1: ANOVA analysis for quadratic model MB photodegradation; Figure S4: Optimized conditions and validation experiment; Equations (S1)–(S4): zero, half, first and second order kinetic models; Figure S5: Kinetic models for (a) zero order, (b), half order, (c) first order, (d) second order; Figure S6: Mechanism of photocatalytic degradation of MB dye by Al_2O_3-MgO, Table S3: Mechanism of photocatalytic degradation of MB dye by Al_2O_3-MgO, Equation (S5): amortization cost; Equation (S6): annual cost.

Author Contributions: Conceptualization, S.D. and A.A.; methodology, S.D.; software, A.A.; validation, S.D.; formal analysis, S.D.; investigation, S.D.; resources, M.N., A.A. and S.O.; data curation, S.D.; writing—original draft preparation, S.D.; writing—review and editing, A.A. and M.N.; visualization, S.D.; supervision, M.N., A.A. and S.O.; project administration, A.A. and M.N. All authors have read and agreed to the published version of the manuscript.

Funding: This research received no external funding.

Data Availability Statement: The data presented in this study are available upon request from the corresponding author.

Acknowledgments: The authors wish to acknowledge TICAD 7 for the scholarship of the researcher as well as JICA and E-JUST for all equipment used throughout the research.

Conflicts of Interest: The authors declare no conflict of interest.

References

1. Khan, I.; Saeed, K.; Zekker, I.; Zhang, B.; Hendi, A.H.; Ahmad, A.; Ahmad, S.; Zada, N.; Ahmad, H.; Shah, L.A.; et al. Review on Methylene Blue: Its Properties, Uses, Toxicity and Photodegradation. *Water* **2022**, *14*, 242. https://doi.org/10.3390/w14020242.
2. Hamdy, A.; Mostafa, M.; Nasr, M. Zero-valent iron nanoparticles for methylene blue removal from aqueous solutions and textile wastewater treatment, with cost estimation. *Water Sci. Technol.* **2018**, *78*, 367–378. https://doi.org/10.2166/wst.2018.306.
3. Safo, K.; Noby, H.; Matatoshi, M.; Naragino, H.; El-Shazly, A.H. Statistical optimization modeling of organic dye photodegradation process using slag nanocomposite. *Res. Chem. Intermed.* **2022**, *48*, 4183–4208. https://doi.org/10.1007/s11164-022-04807-5.
4. Abdelhaleem, A.; Chu, W. Photodegradation of 4-chlorophenoxyacetic acid under visible LED activated N-doped TiO 2 and the mechanism of stepwise rate increment of the reused catalyst. *J. Hazard. Mater.* **2017**, *338*, 491–501. https://doi.org/10.1016/j.jhazmat.2017.05.056.

5. Ateş, S.; Baran, E.; Yazıcı, B. The nanoporous anodic alumina oxide formed by two-step anodization. *Thin Solid Film.* **2018**, *648*, 94–102. https://doi.org/10.1016/j.tsf.2018.01.013.
6. Mebed, A.M.; Abd-Elnaiem, A.M.; Alshammari, A.H.; Taha, T.A.; Rashad, M.; Hamad, D. Controlling the Structural Properties and Optical Bandgap of PbO–Al_2O_3 Nanocomposites for Enhanced Photodegradation of Methylene Blue. *Catalysts* **2022**, *12*, 142. https://doi.org/10.3390/catal12020142.
7. Bin Mokaizh, A.A.; Shariffuddin, J.H.B.H. Manufacturing of Nanoalumina by Recycling of Aluminium Cans Waste. In *Waste Recycling Technologies for Nanomaterials Manufacturing*; Topics in Mining, Metallurgy and Materials Engineering; Makhlouf, A.S.H., Ali, G.A.M., Eds.; Springer International Publishing: Cham, Switzerland, 2021; pp. 851–870. https://doi.org/10.1007/978-3-030-68031-2_30.
8. Bharthasaradhi, R.; Nehru, L. Structural and phase transition of α-Al_2O_3powders obtained by co-precipitation method. *Phase Transitions* **2016**, *89*, 77–83. https://doi.org/10.1080/01411594.2015.1072628.
9. Mantilaka, M.P.G.; De Silva, R.T.; Ratnayake, S.P.; Amaratunga, G.; de Silva, K.N. Photocatalytic activity of electrospun MgO nanofibres: Synthesis, characterization and applications. *Mater. Res. Bull.* **2018**, *99*, 204–210. https://doi.org/10.1016/j.materresbull.2017.10.047.
10. Makuła, P.; Pacia, M.; Macyk, W. How To Correctly Determine the Band Gap Energy of Modified Semiconductor Photocatalysts Based on UV−Vis Spectra. *J. Phys. Chem. Lett.* **2018**, *9*, 6814–6817. https://doi.org/10.1021/acs.jpclett.8b02892.
11. Hassena, H. Photocatalytic Degradation of Methylene Blue by Using Al2O3/Fe2O3 Nano Composite under Visible Light. *Mod. Chem. Appl.* **2016**, *2016*, 1000176. https://doi.org/10.4172/2329-6798.1000176.
12. Salazar-Rabago, J.J.; Leyva-Ramos, R.; Rivera-Utrilla, J.; Ocampo-Perez, R.; Cerino-Cordova, F.J. Biosorption mechanism of Methylene Blue from aqueous solution onto White Pine (*Pinus durangensis*) sawdust: Effect of operating conditions. *Sustain. Environ. Res.* **2017**, *27*, 32–40. https://doi.org/10.1016/j.serj.2016.11.009.
13. Allawi, F.; Juda, A.M.; Radhi, S.W. Photocatalytic degradation of methylene blue over MgO/α-Fe2O3 nano composite prepared by a hydrothermal method. **2020**, *2290*, 030020. https://doi.org/10.1063/5.0029461.
14. Vinothkumar, P.; Manoharan, C.; Shanmugapriya, B.; Bououdina, M. Effect of reaction time on structural, morphological, optical and photocatalytic properties of copper oxide (CuO) nanostructures. *J. Mater. Sci. Mater. Electron.* **2019**, *30*, 6249–6262. https://doi.org/10.1007/s10854-019-00928-7.
15. Mensah, K.; Samy, M.; Ezz, H.; Elkady, M.; Shokry, H. Utilization of iron waste from steel industries in persulfate activation for effective degradation of dye solutions. *J. Environ. Manag.* **2022**, *314*, 115108. https://doi.org/10.1016/j.jenvman.2022.115108.

Proceedings

Fabrication of aluminum-based hybrid nanocomposite for photocatalytic degradation of methylene blue dye: A techno-economic approach †

Samuel Demarema [1], Amal Abdelhaleem [1]*, Shinichi Ookawara [2], and Mahmoud Nasr [1,3]*

[1] Environmental Engineering Department, Egypt-Japan University of Science and Technology (E-JUST), Alexandria, 21934, Egypt; *amal.elsonbaty@ejust.edu.eg
[2] Department of Chemical Science and Engineering, Tokyo Institute of Technology, Meguro-ku, Tokyo, 152-8552, Japan; ookawara.s.aa@m.titech.ac.jp
[3] Sanitary Engineering Department, Faculty of Engineering, Alexandria University, Alexandria, 21544, Egypt; Mahmoud.Nasr@just.edu.eg
Correspondence: samuel.demarema@ejust.edu.eg

Supplementary Data

1.1 Synthesis method

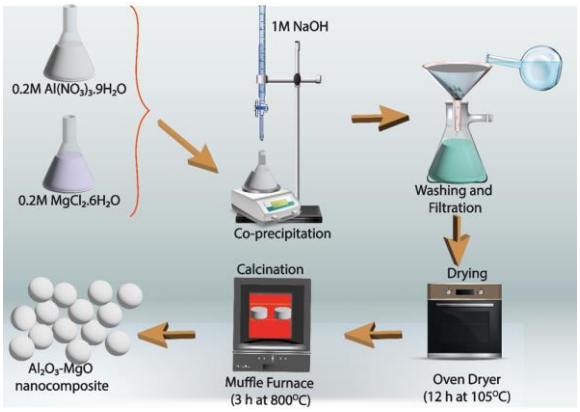

Figure S1: Synthesis of Al_2O_3-MgO

1.2 Point of zero charge of Al_2O_3-MgO

The point of zero charge was determined using batch equilibrium method [4]. 50 ml of 0.1 M NaCl was prepared, and the pH adjusted using 1M NaOH or 1M H_2SO_4. 0.1 g of Al_2O_3-MgO was added and the suspension was stirred for 24 hours in an orbital shaker. Figure S2 shows the pH_{zc} of Al_2O_3-MgO as 10.04.

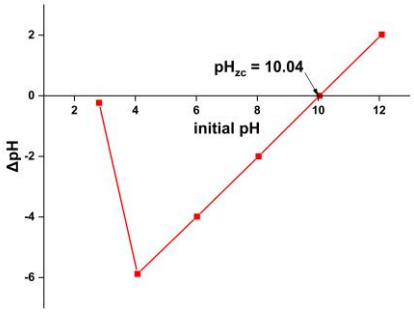

Figure S2. pH_{zc} of Al_2O_3-MgO.

Citation: To be added by editorial staff during production.

Academic Editor: Firstname Lastname

Published: date

1.3 Interaction of parameters

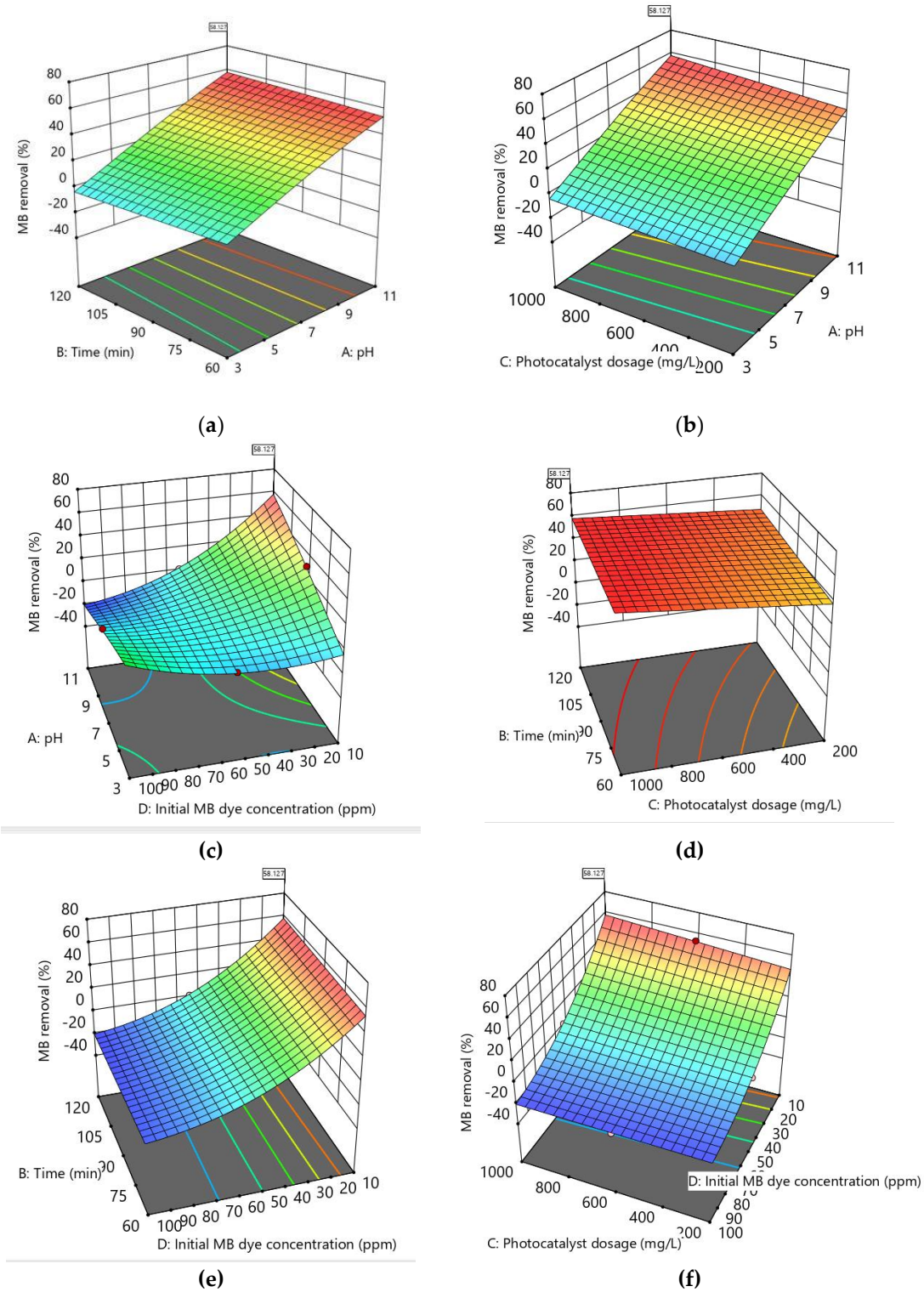

Figure S3. 3D contour plots for interaction of: (**a**) pH with time; (**b**) pH and photocatalyst dosage; **(c)** pH and initial dye concentration; **(d)** photocatalyst dosage and time; **(e)** initial MB dye concentration and time; **(f)** photocatalyst dosage and initial MB dye concentration.

1.4 Optimization and validation

The ANOVA analysis for the quadratic model is shown in Table S1.

Table S1 ANOVA analysis for quadratic model MB photodegradation

Source	Sum of Squares	df	Mean Square	F-value	p-value	
Model	1029.44	14	73.53	81.99	< 0.0001	significant
A-pH	29.26	1	29.26	32.63	< 0.0001	
B-Time	11.41	1	11.41	12.73	0.0031	
C-Photocatalyst dosage	2.46	1	2.46	2.74	0.1198	
D-Initial MB dye concentration	348.8	1	348.8	388.92	< 0.0001	
AB	15.5	1	15.5	17.29	0.001	
AC	0.5407	1	0.5407	0.6029	0.4504	
AD	412.34	1	412.34	459.77	< 0.0001	
BC	4.39	1	4.39	4.9	0.0441	
BD	8.2	1	8.2	9.14	0.0091	
CD	4.11	1	4.11	4.59	0.0503	
A^2	12.29	1	12.29	13.7	0.0024	
B^2	0.0067	1	0.0067	0.0074	0.9325	
C^2	0.0006	1	0.0006	0.0006	0.9804	
D^2	152.97	1	152.97	170.57	< 0.0001	
Residual	12.56	14	0.8968			
Lack of Fit	10.6	10	1.06	2.17	0.2372	not significant
Pure Error	1.96	4	0.489			
Cor Total	1042	28				

R^2 = 0.998, R^2(adj) = 0.9759

The optimized conditions are shown in Fig S3a. A validation experiment was carried out using the optimized conditions and the result is shown in Figure S2b.

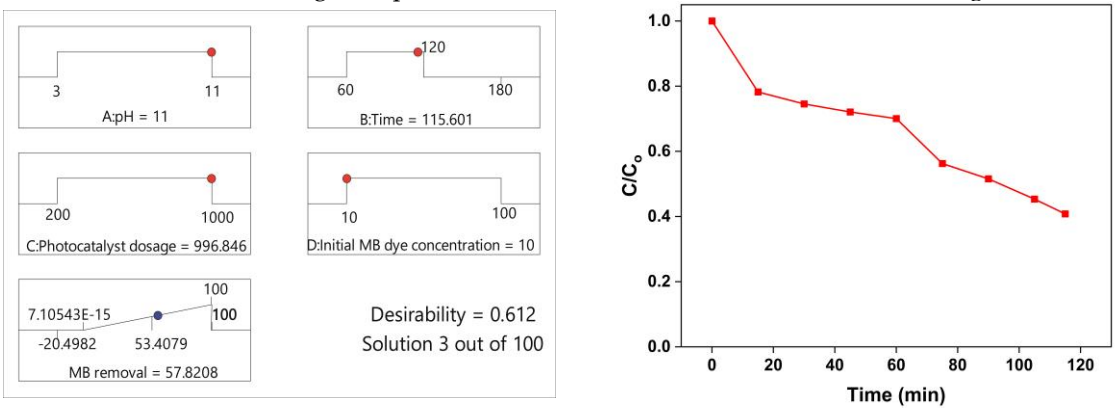

(**a**) (**b**)

Figure S4. (**a**) Optimized conditions and (**b**) Result of validation experiment

1.5 Photodegradation kinetics

The photocatalytic degradation of MB using Al_2O_3-MgO was studied at optimized conditions using kinetic models. Zero order (Equation S1), half order (Equation S2), first order (Equation S3) and second order (Equation S4) kinetic models were used.

$$C_t = C_o - k_o t \quad \text{(S1)}$$

$$C_t\text{^}(1/2) = C_o\text{^}(1/2) - (k_{0.5}/2)t \quad \text{(S2)}$$

$$\ln C_t = \ln C_o - k_1 t \quad \text{(S3)}$$

$$1/C_t = 1/C_o + k_2 t \quad \text{(S4)}$$

Where C_o is initial MB concentration, C_t is concentration of MB at time t. k_0, $k_{0.5}$, k_1, and k_2 are the respective rate constants for zero, half, first and second order kinetic models [11]. Figure S4 shows the kinetic modelling results.

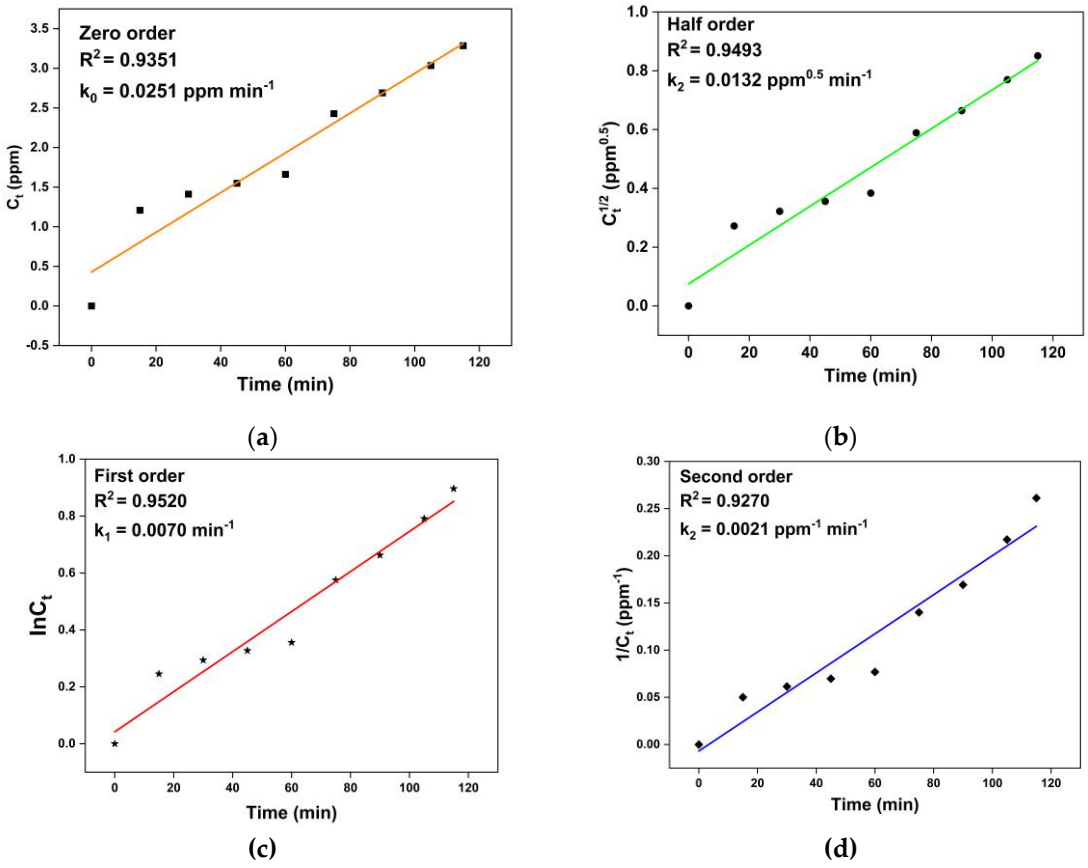

Figure S5. Kinetic models for **(a)** zero order, **(b)**, half order, **(c)** first order, **(d)** second order

1.6 Suggested mechanism

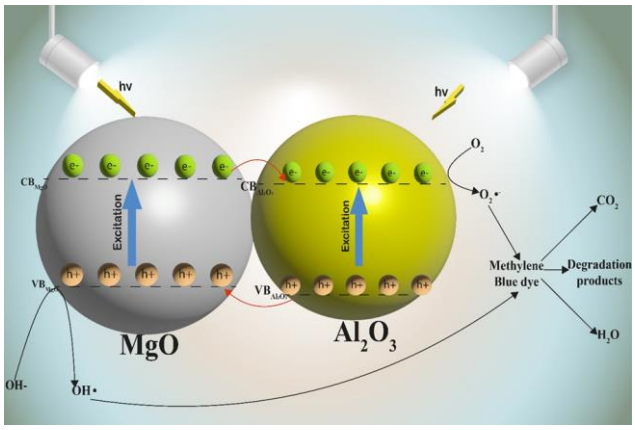

Figure S6. Mechanism of photocatalytic degradation of MB dye by Al_2O_3-MgO.

1.7 Economic evaluation

Table S3 shows the capital (CAPEX) and operating (OPEX) costs for synthesis and application of Al_2O_3-MgO nanocomposite in photodegradation of textile wastewater.

Table S3 CAPEX and OPEX

Item	Description	%	Amount (USD)
Capital Cost (OPEX)			
Purchased Equipment Cost (PCE)	Total cost of all process equipment (photoreactor, dryer, filtration units)	21	818,250
Installation, piping, instrumentation, and control	Power supply infrastructure for plant	13	506,535.71
Electrical systems		6	233,785.71
Land, buildings, and yard services		20	77,928.57
Indirect Costs		14	545,500
Contractor's fee and contingency		11	428,607.14
Working Capital		15	584,464.28
CAPEX		**100**	**3,896,428.57**
Operational costs (OPEX)			
Variable Costs			
Raw materials	Al(NO3)3.9H2O, MgCl2.6H2O, chemicals (bases, acids), water	52	15,730
Electricity	Power supply to photoreactor, Powering mechanical mixers	15	4,537.50
Miscellaneous costs	Replacing UV lamps in photoreactor, changing catalyst holders, changing reactor linings,	10	3,025
Fixed Costs			
Labor	Renumeration for all plant personnel in general operation and maintenance of wastewater treatment plant	15	4,537.50
Analytical Costs	Expenses in wages for laboratory personnel, water sampling costs,	3	907.50
Maintenance and insurance		5	1512.50
OPEX		**100**	**30,250**

The amortization cost is calculated using Equation S5.

$$A = (1.2 \times CAPEX \times r) / [1-(1/1+r)^n] \quad (S5)$$

Where n is the number of operational years of the wastewater treatment plant, at 25 and r is the interest rate at 6%. The annual cost (AC) of treating textile wastewater cost per m^3 of treating textile wastewater was evaluated using Equation 9.

$$AC = (OPEX + A) / \text{annual volume of wastewater treated} \quad (S6)$$